

Soft-X-ray Emission Studies of Buried Interfaces in Multilayers

Takashi Imazono,* Noboru Miyata** and Mihiro Yanagihara
Institute of Multidisciplinary Research for Advanced Materials, Tohoku University
2-1-1 Katahira, Aoba-ku, Sendai 980-8577, Japan
Fax: 81-22-217-5379, e-mail: m.yanagi@tagen.tohoku.ac.jp

By the curve fitting analysis for the Si $L_{2,3}$ emission spectra measured for Mo/Si and Fe/Si multilayers, chemical composition and thickness of the interdiffusion layers were estimated within an error of 0.1 nm. An FeSi₂ layer of 0.7 nm thick was found to be sandwiched with Fe₃Si layers for the antiferromagnetically coupled Fe/Si multilayer. Besides, using total reflection technique a SiO₂ layer was found at the topmost Fe₃Si layer in Fe/Si multilayers. The soft-X-ray emission spectroscopy was confirmed to have high potential to analyze buried interfaces nondestructively.

Key words: soft X-ray emission, buried interface, interdiffusion, multilayer, total reflection

1. INTRODUCTION

As novel devices, multilayers or superlattices have recently attracted much interest. For further development it is quite essential to understand the structure and chemical composition of the interfaces. They have been usually studied by X-ray diffraction and Rutherford backscattering spectroscopy nondestructively, or otherwise by Auger depth profiling and transmission electron microscopy destructively. As a novel approach soft-X-ray emission (SXE) spectroscopy is expected to be a useful tool to study buried layers and interfaces. Because the mean free path of soft X-rays is a few tens nm, even if the objects are covered by thin films of other materials, SXE from the buried objects suffers slight loss in intensity from absorption. Moreover, the SXE spectrum reflects sensitively the partial density of state of valence band due to the dipole transition and the flat core levels. These properties enable us to obtain information of the buried objects nondestructively. Recent advances in synchrotron radiation technology have made it possible to measure SXE spectra from buried objects by using intense monochromatized soft X-rays. Excitation near the absorption threshold makes it possible to excite the objective element selectively, and thus to measure the SXE spectra effectively. The SXE spectra do not suffer higher order spectra from other constituent elements, which is sometimes serious obstruction for the electron-beam SXE spectroscopy.

In this paper our SXE studies for the interfaces in Mo/Si and Fe/Si multilayers are described [1,2]. In addition, our recent result of total-reflection SXE spectroscopy applied for Fe/Si multilayers is also presented [3]. From the results, it will be shown that the SXE spectroscopy is a promising tool to study the buried interdiffusion layers and interfaces. Mo/Si multilayer mirrors are useful optical components in the 100 eV energy region. They are used as high-reflectivity normal-incidence mirrors, polarizers, phase shifters and

beam splitters. It has been expected to apply them to soft-X-ray microscopes, interferometers, projection lithography, *etc.* Concerning the Mo/Si multilayers, it is known that interdiffusion occurs at the interface region between the Mo and Si layers. This interdiffusion causes the multilayer to degrade the optical quality. Until now, the interdiffusion layer has been studied by the usual methods, and has been concluded to consist of MoSi₂ [4]. It should be also examined using SXE spectroscopy. To understand exactly the interface enables us to improve the performance of soft-X-ray multilayers.

Fe/Si multilayers have attracted our attention for the strong magnetic interlayer coupling with thin Si spacers. Since the discovery of giant magnetoresistance in 1988, magnetic multilayers have attracted much interest from the viewpoint of basic research in the solid state physics as well as industrial applications such as magnetic sensors and heads. The giant magnetoresistance is based on magnetic interlayer coupling between ferromagnetic layers. For the origin of the magnetic interaction in the Fe/Si system, several models have been proposed. The key point of the problem is the severe interdiffusion at the interfaces and thus the complex diffused structure of the Si spacer. Interdiffusion at the interface throughout layer deposition is to some extent avoidable by high-speed deposition. Endo, Kitakami, and Shimada [5] deposited Fe/Si multilayers at a high rate, and achieved a drastic enhancement in the interlayer coupling. However, the kind of the silicide that mediates the interlayer coupling and thus the origin of the enhancement have been an open question yet.

Total-reflection X-ray fluorescence analysis yields information on the ratio of constituent elements in the surface region. Moreover, by changing the angle of incidence, we can obtain a depth profile of element distribution nondestructively. We expect that the SXE spectroscopy coupled with a technique of photon incidence at a critical angle of total reflection may be a

* Present address: Kansai Research Establishment, JAERI, 8-1 Umemidai, Kizu-cho, Souraku-gun, Kyoto 619-0215, Japan, e-mail: imazono@apr.jaeri.go.jp.

** Present address: Industrial Technology Institute, Miyagi Prefecture, 2-2 Akedouri, Izumi-ku, Sendai 981-3116, Japan e-mail: nmiyata@mit.pref.miyagi.jp.

useful tool to study the chemical state near the surface of materials. The evanescent wave enhances the SXE from the vicinity of surface. The critical angle of total reflection for a sample at soft X-ray wavelengths is larger than at hard X-ray wavelengths. It is thus easier to adjust a sample to a critical angle of incidence for soft X-rays than hard X-rays. Moreover, the light elements can be dealt with in the soft X-ray region.

2. EXPERIMENTAL

The SXE experiments were carried out using synchrotron radiation at BL- 3B, 12A, and 16B of the Photon Factory. The SXE spectrometer [6] used in our study was a flat-field type on the basis of a 1200-grooves/mm grating with a 5.6-m radius of curvature (Hitachi, 001-0437). As the position-sensitive detector a resistive-anode type X-ray detector (Quantar Tech., 3391A) was employed. The slit width was fixed at 0.1 mm, and the resolution was about 0.4 eV at 100 eV. The angle of incidence of the primary photons for the sample was usually 60° with regard to the sample normal except for the total-reflection measurement. Si $L_{2,3}$ emission spectra were recorded for the multilayers and reference samples at incident energies above 120 eV.

For the spectral analysis to estimate the layer thickness, we made several assumptions. One is that the incident beam intensity changes negligibly small along an interdiffusion layer. This assumption is reasonable because the beam actually penetrates through at least 10 bilayers even for the largest t multilayer. The other is that the Si atoms absorb primary photons at an equal rate independent of the chemical state, that is, the kind of silicide. The assumption is reasonable except for excitation near the absorption edge. Moreover, the rate of the Si $L_{2,3}$ emission is assumed to be the same independent of the chemical state. Thus the emission intensity is proportional to the total number of Si atoms in each silicide layer. If the emission spectrum for a silicide is normalized with the density of Si atoms, the emission intensity is proportional to the thickness of the silicide layer [1]. If the silicide layer gradates toward another silicide at the interfaces, the obtained thickness means an effective one including half the gradation layers. Curve fitting analysis was carried out using the nonlinear least squares method based on the Levenberg-Marquardt algorithm.

3. RESULTS AND DISCUSSION

3.1 Mo/Si Multilayers

Five Mo/Si multilayer samples were grown to 15 bilayers on Si wafers using a magnetron sputter system. The Mo layer was constant to be 3.4 nm in thickness for each sample, while the Si layer was 0.5 nm, 1.2 nm, 2.8 nm, 5.9 nm, and 13.3 nm for the respective samples. The topmost layer was Mo. A 100-nm-thick amorphous Si (*a*-Si) single layer was also prepared using the same sputter system. To eliminate emission from the Si wafer, a 100-nm-thick Mo buffer layer was deposited prior to each sample deposition. In addition, MoSi_2 , Mo_5Si_3 , and Mo_3Si were commercially obtained as reference samples. The SXE experiment was carried out at BL 12A. The energy band of the excitation light was 4 eV, and that of the spectrometer was 1.0 eV at 90 eV in this case.

Figure 1 shows the Si $L_{2,3}$ emission spectra measured

for the Mo/Si multilayers and *a*-Si, where the number indicates the Si-layer thickness in nm. The main peak at 90 eV becomes sharper with decreasing Si thickness. Spectrum E is quite similar to that for *a*-Si. This suggests that most of the Si layer in sample E is amorphous, and that the contribution of the interface region to the SXE spectrum becomes dominant for the thin Si-layer samples.

Figure 2 shows the Si $L_{2,3}$ emission spectra for MoSi_2 , Mo_5Si_3 , and Mo_3Si . As is shown, the feature of the spectrum A in Fig. 1 is very close to that of Mo_3Si . This is an evidence for the interface to consist of Mo_3Si . The spectra B, C and D were reproduced using the spectra of *a*-Si and Mo_3Si with an appropriate ratio. From the fitting analysis thickness of the Mo_3Si layer was estimated to be 0.77, 0.84 and 0.81 nm for B, C and D, respectively. Assuming that the interdiffusion layer is

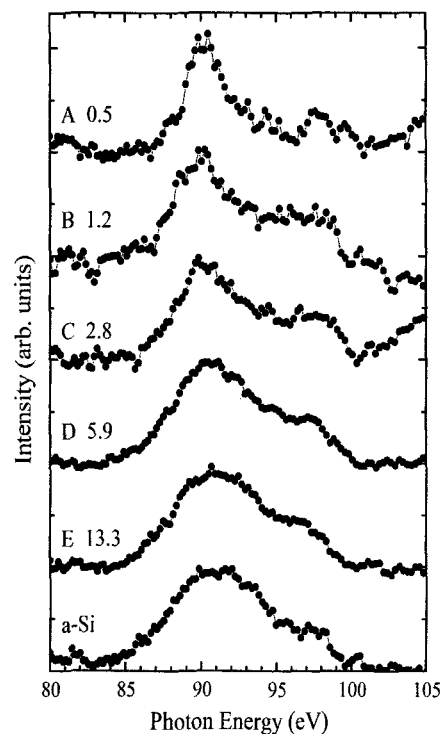


Fig. 1. Si $L_{2,3}$ emission spectra measured for the Mo/Si multilayers and amorphous Si.

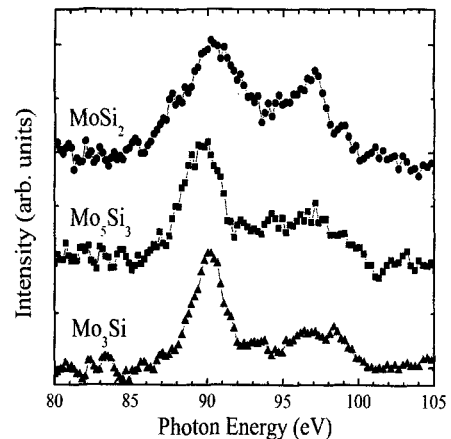


Fig. 2. Si $L_{2,3}$ emission spectra measured for MoSi_2 , Mo_5Si_3 , and Mo_3Si .

the same among the multilayers, the thickness is $0.8 \text{ nm} \pm 0.1 \text{ nm}$. It is shown that the chemical state of the interdiffusion layer can be estimated within an error of 0.1 nm using SXE spectroscopy. Although the S/N ratio of the measured spectra was not high, the precision in thickness estimation was very high in this case. The most probable reason is that only Mo_3Si was present at the interface region. It is reported that the interdiffusion layer is different between the interfaces of Si on Mo and Mo on Si. The SXE spectroscopy yields an averaged thickness for such case.

3.2 Fe/Si Multilayers

Seven $\text{Fe/Si}(t)$ multilayer samples were grown to 22 bilayers using a dc magnetron sputter system. Thickness of the Fe layer was fixed at 3.0 nm and that of the Si layer t varied from 0.5 to 3.0 nm for respective samples. The deposition rates were 0.20 and 0.07 nm/s for Fe and Si layers, respectively. Crystallographic structures of the Fe/Si multilayers were examined using X-ray diffraction. Magnetic and electric properties of the multilayers were also examined. Magnetic interlayer coupling of the multilayers changed with t , *i.e.*, first ferromagnetic for $t = 0.5 \text{ nm}$, then antiferromagnetic for $t = 1.0, 1.3, \text{ and } 1.5 \text{ nm}$, next ferromagnetic again for $t = 1.7 \text{ nm}$, and finally noncoupling for $t = 2.0$ and 3.0 nm . The strongest antiferromagnetic (AF) coupling was observed for the $\text{Fe/Si}(1.3 \text{ nm})$ multilayer.

The SXE experiment was carried out using undulator radiation at BL 16B. Figure 3 shows the Si $L_{2,3}$ emission spectra measured for the $\text{Fe/Si}(t)$ multilayers. They exhibit commonly a main peak at about 90 eV and a shoulder around 98 eV , which are associated with the nonbonding Si $3s$ and Fe $3d$ orbitals, respectively. The

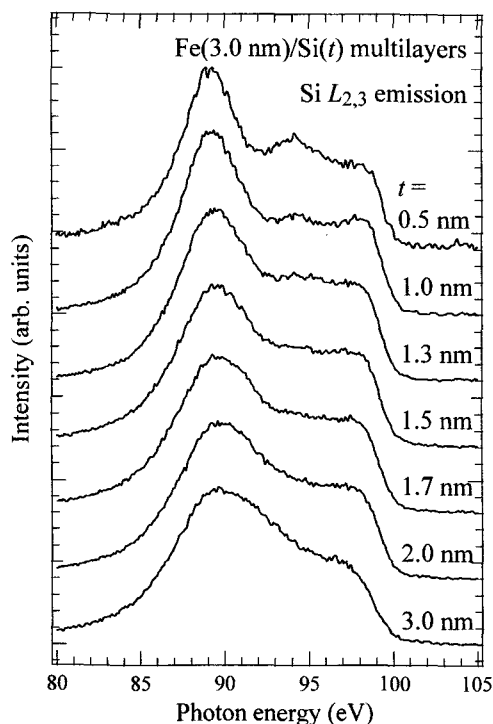


Fig. 3. Si $L_{2,3}$ emission spectra measured for the $\text{Fe/Si}(t)$ multilayers.

spectrum of the $\text{Fe/Si}(3.0 \text{ nm})$ multilayer is very similar to that for $a\text{-Si}$ shown in Fig. 1. The spectral feature changes considerably with t . As similar to the Mo/Si multilayers, the influence of the silicides in the interdiffusion layer becomes more dominant for multilayers of smaller t .

According to the phase diagram of the Fe-Si system, Fe_3Si , FeSi , and FeSi_2 are stable at room temperature. When using emission spectra of crystalline Fe_3Si , FeSi , and FeSi_2 , and $a\text{-Si}$, the degree of curve fitting was quite insufficient. The most probable reason for the disagreement is that the interdiffusion layer is also amorphous as the initial Si layer is amorphous. For exact discussion, the interdiffusion layer should be analyzed with Fe-Si compounds grown by the same magnetron sputter deposition. We thus prepared seven $\text{Fe}_{1-x}\text{Si}_x$ alloy single layers on Si wafers to about 100 nm thick. All the alloy and Si single layers were ascertained to be amorphous. The content was determined using X-ray photoelectron spectroscopy. As it was difficult to achieve exactly $x = 0.25, 0.5, \text{ and } 0.67$ for Fe_3Si , FeSi , and FeSi_2 , respectively, we obtained Si $L_{2,3}$ emission spectra for $a\text{-Fe}_3\text{Si}$, FeSi , and FeSi_2 as shown in Fig. 4 by interpolation for the spectra of the $a\text{-Fe}_{1-x}\text{Si}_x$ alloys.

The layer thickness of Fe_3Si , FeSi , FeSi_2 , SiO_2 , and Si was determined for each $\text{Fe/Si}(t)$ multilayer using the emission spectra for these amorphous silicides. Figure 5 shows an example of the curve fitting applied for the AF coupled multilayer. The agreement is quite well. Figure 6 shows the layer thickness per period plotted as a function of the initial Si layer thickness t . Thickness of the interdiffusion layer obtained by adding the thickness of Fe_3Si , FeSi , and FeSi_2 is also shown with open circles. The interdiffusion layer increases from 0.7 nm to 1.7 nm with increasing t from 0.5 nm to 1.3 nm , and is then saturated. The saturated thickness is roughly consistent with that estimated from a TEM image. On the other hand, the Si layer is not found below $t = 1.5 \text{ nm}$, and then increases with increasing t . This result is quite reasonable because the Si layer is wasted completely by chemical combination with Fe atoms for the multilayers of small t , and then the interdiffusion layer becomes constant independent of t for the multilayers of sufficient t . This means also that no more interdiffusion occurs

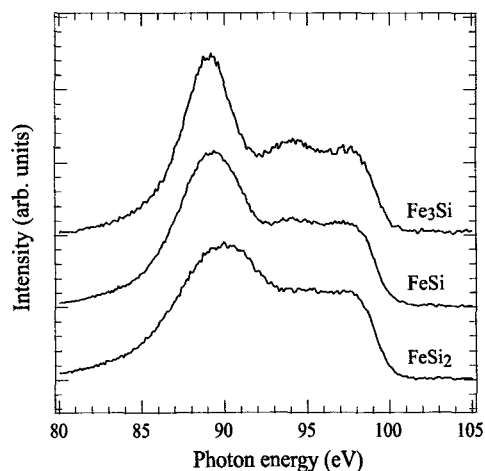


Fig. 4. Si $L_{2,3}$ emission spectra for amorphous Fe_3Si , FeSi , and FeSi_2 .

after layer deposition. However, the α -FeSi₂ and FeSi layers change in thickness alternately above $t = 1.5$ nm, whereas the total interdiffusion layer keeps constant. The reason has not been explained yet. For large t their difference reasonably approaches a constant amount due to the interdiffusion accompanied with chemical combination. Now we discuss the layer composition in terms of the magnetic coupling. In the range from $t = 1.0$ to 1.5 nm, where the multilayer is AF coupled, α -Fe₃Si and FeSi₂ are dominant, whereas α -FeSi and Si are not found. As for the most strongly coupled Fe/Si(1.3nm) multilayer, α -Fe₃Si and FeSi₂ layers are 1.0 nm and 0.7 nm thick, respectively. This is an important result of this study, because the middle layer sandwiched between the

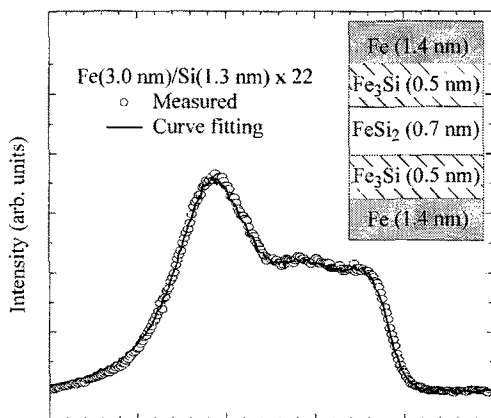


Fig. 5. Curve fitting for the Si $L_{2,3}$ emission spectrum of the Fe/Si(1.3nm) multilayer. The layer structure obtained from the analysis is also shown in the insert.

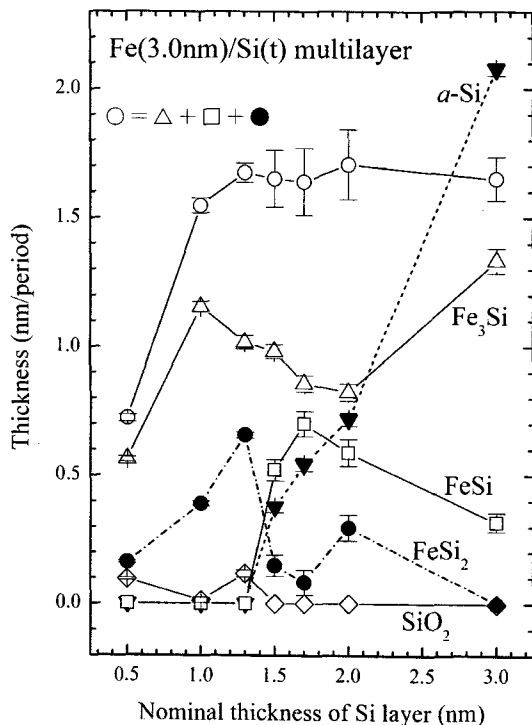


Fig. 6. Plots of the thickness per period of each layer determined for each Fe/Si(t) multilayer.

Fe₃Si layer has been definitely assigned to α -FeSi₂ of 0.7 nm thick, as shown in the insert of Fig. 5. The α -Fe₃Si is metallic and ferromagnetic, while α -FeSi₂ is insulating and nonmagnetic. Because the strong interlayer coupling originates from a layer structure of ferromagnetic/nonmagnetic, the presence of α -FeSi₂ is quite reasonable and would play an important role in the strong AF coupling of the multilayer. As α -FeSi₂ is not metallic, the quantum interference model [7] is the most suitable for the interlayer coupling. Actually, the interlayer-coupling constant was estimated for a system with an FeSi₂ layer of 0.7 nm thick to be 1.5 erg/cm², which agrees well with 1.2 erg/cm² obtained by Endo *et al.* [5]. The result that the α -FeSi₂ spacer mediates the interlayer coupling suggests a practical approach to achieve high quality Fe/Si multilayers.

3.3 Total-reflection SXE Spectroscopy

As is shown in Fig. 6, SiO₂ was slightly found in the Fe/Si multilayers. However, its site has been unknown yet. We applied total-reflection SXE spectroscopy for three Fe/Si(t) multilayers of $t = 1.0, 1.3,$ and 1.5 nm to clarify this point. SXE experiment was carried out at BL 3B. The excitation energy was fixed at 155 eV. The critical angle of total reflection of Fe for $E = 155$ eV is 76.3°. In this case, penetration depth is estimated to be about 4 nm. The angles of incidence of the excitation light θ we chosen were 60° and 76°. When $\theta = 60^\circ$, the penetration depth is about 15 nm for Fe and 22 nm for Si. Therefore, at least four or five layer periods might be probed by incident soft X-rays considering the Fe layer.

Figure 7 shows the Si $L_{2,3}$ emission spectra measured for the Fe/Si multilayers for $\theta = 60^\circ$ and 76° , which are indicated with the solid and dotted lines, respectively. It is remarkable that the spectra for $\theta = 76^\circ$ have a structure at 94 eV as compared with those for $\theta = 60^\circ$. It originates from SiO₂. Effective thickness of each layer was estimated by curve fitting analysis using the SXE spectra for α -Fe₃Si, FeSi, FeSi₂, Si, and SiO₂. The t

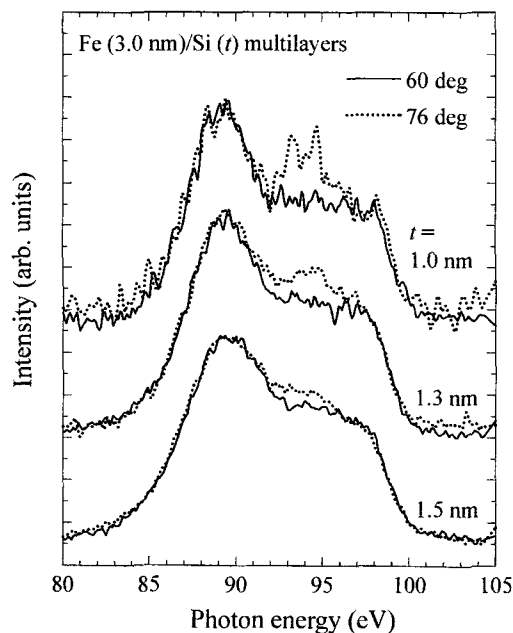


Fig. 7. Si $L_{2,3}$ emission spectra measured for Fe/Si(t) multilayers for $\theta = 60^\circ$ (solid) and 76° (dotted).

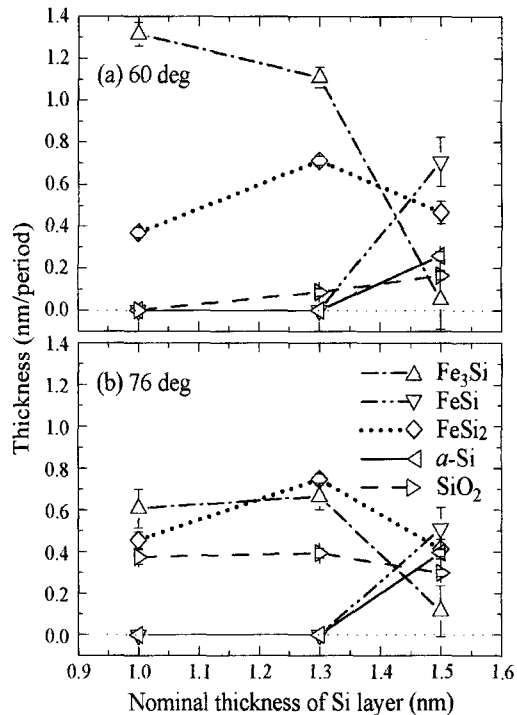


Fig. 8. Plots of the thickness of each layer per period determined for each $\text{Fe/Si}(t)$ multilayer for $\theta = 60^\circ$ (a) and 76° (b).

dependence of the layer thickness concerning the spectra for $\theta = 60^\circ$ and 76° is summarized in Figs. 8(a) and 8(b), respectively. As for the case of $\theta = 60^\circ$ the t dependence is basically consistent with what described in the previous section. Fe_3Si and FeSi_2 are dominant, while FeSi , $\alpha\text{-Si}$, and SiO_2 are minor, particularly for the $t = 1.0$ and 1.3 nm samples. Among them, FeSi_2 has been concluded to mediate the antiferromagnetic coupling, as mentioned above. As compared with the case of $\theta = 60^\circ$, there is remarkable change in the layer thickness with regard to Fe_3Si and SiO_2 , while almost no change is found for FeSi , FeSi_2 , and $\alpha\text{-Si}$ for the case of $\theta = 76^\circ$. Therefore, we will discuss the change observed for Fe_3Si and SiO_2 . In comparison with the case of $\theta = 60^\circ$, the layer thickness of SiO_2 remarkably increased from a negligibly small thickness to 0.38 nm when $\theta = 76^\circ$ for the samples of $t = 1.0$ and 1.3 nm. On the contrary, thickness of the Fe_3Si layer decreased from 1.3 nm to 0.60 nm for the $t = 1.0$ nm sample and it decreased also from 1.1 nm to 0.66 nm for the $t = 1.3$ nm sample. The depth probed when $\theta = 76^\circ$ is within about 4 nm from the surface. The layer structure illustrated in Fig. 5 should be referred. It may be said that primarily the silicide layers close to the topmost Fe layer was probed. It is thus concluded that the SiO_2 layer of 0.4 nm thick locates between the topmost Fe and Fe_3Si layers, because the SiO_2 layer was generated by oxidation of the Fe_3Si layer close to the topmost Fe layer. Consequently, the topmost Fe_3Si layer reduces in thickness from 0.5 nm to 0.1 nm, whereas the second Fe_3Si layer was not oxidized, as is found in Fig. 8(b). It is the most probable that the oxidation started from the surface when the sample was exposed to the atmosphere. The topmost Fe layer was also oxidized, but not detected in this study.

The SiO_2 layer was also observed when $\theta = 60^\circ$. However, its thickness was estimated to be very small, because SiO_2 was also assumed to distribute regularly over the multilayer in the fitting analysis. The result concerning the site of SiO_2 was also supported by XPS analysis that the Si $2p$ peaks due to SiO_2 disappeared after ion etching. These results also mean that the interdiffusion model we have employed is quite adequate because Fe_3Si layer is the nearest to the topmost Fe layer among the silicides. Finally, the result in this study suggests that the total-reflection SXE spectroscopy is a promising tool to analyze the bonding state of constituent elements within a depth of a few nanometers from the surface. Moreover, the SXE technique is able to deal with the light elements such as Be, B, C, N, and O. This is also an advantage of the SXE spectroscopy.

4. CONCLUSIONS

Si $L_{2,3}$ emission spectra were measured for magnetron sputtered Mo/Si and Fe/Si multilayers. By the curve fitting analysis, chemical composition of the interdiffusion layer and the thickness was estimated within an error of 0.1 nm. For the Mo/Si multilayers, a Mo_3Si layer of 0.8 nm thick was found for the first time. An $\alpha\text{-FeSi}_2$ layer of 0.7 nm thick was found to be sandwiched with $\alpha\text{-Fe}_3\text{Si}$ layers for the most strongly coupled Fe/Si multilayer. The FeSi_2 layer was interpreted to be active in the magnetic coupling using a quantum interference model. Besides, using a total-reflection technique with the emission spectroscopy SiO_2 layer was confirmed to locate near the surface of the Fe/Si multilayers. From these results the SXE spectroscopy was confirmed to have potential abilities as a tool to analyze buried interfaces and interdiffusion layers nondestructively.

Acknowledgments

The authors would like to thank Prof. M. Watanabe, Prof. O. Kitakami and Prof. Y. Shimada for their fruitful discussion. They also thank S. Ishikawa, Y. Hirayama, S. Ichikura, and K. Sudo for their cooperation in the SXE experiments. This work was supported in part by the Mitsubishi Foundation.

References

- [1] N. Miyata, S. Ishikawa, M. Yanagihara and M. Watanabe, *Jpn. J. Appl. Phys.* **38**, 6476-78 (1999).
- [2] T. Imazono, N. Miyata, O. Kitakami, and M. Yanagihara, *Surf. Rev. Lett.* **9**, 669-72 (2002); T. Imazono *et al.*, *Photon Factory Activity Report 2001*, Part B, 56 (2003); to be submitted to *Jpn. J. Appl. Phys.*
- [3] T. Imazono *et al.*, to be published in *Photon Factory Activity Report 2002*, Part B (2003); to be submitted to *Jpn. J. Appl. Phys.*
- [4] J. M. Slaughter, A. Shapiro, P. A. Kearney and C. M. Falco, *Phys. Rev.* **B 44**, 3854 (1991).
- [5] Y. Endo, O. Kitakami, and Y. Shimada, *Phys. Rev.* **B 59**, 4279 (1999).
- [6] M. Yanagihara, Y. Goto, N. Miyata, and M. Furudate, *Rev. Sci. Instrum.* **66**, 1595 (1995).
- [7] P. Bruno, *J. Appl. Phys.* **76**, 6972 (1994).

(Received July 21, 2003; Accepted August 21, 2003)